CRYSTAL GROWTH & DESIGN

Article

pubs.acs.org/crystal

A Fluorinated Metal–Organic Framework for High Methane Storage at Room Temperature

Ganggang Chang,[†,‡] Huimin Wen,[‡] Bin Li,[*,‡] Wei Zhou,[§] Hailong Wang,[‡] Khalid Alfooty,[∥] Zongbi Bao,[*,†,‡] and Banglin Chen[*,‡,∥]

[†]Key Laboratory of Biomass Chemical Engineering of Ministry of Education, College of Chemical and Biological Engineering, Zhejiang University, Hangzhou 310027, China

[‡]Department of Chemistry, University of Texas at San Antonio, One UTSA Circle, San Antonio, Texas 78249-0698, United States

[§]NIST Center for Neutron Research, National Institute of Standards and Technology, Gaithersburg, Maryland 20899-6102, United States

[∥]Department of Chemistry, Faculty of Science, King Abdulaziz University, Jeddah 22254, Saudi Arabia

Supporting Information

ABSTRACT: A fluorinated metal–organic framework NOTT-108 with single pure-phase has been synthesized for the first time, which has enabled us to examine the effect of the substituted fluorine atoms on the methane storage. The activated NOTT-108a shows a permanent porosity comparable to its isoreticular NOTT-101a but exhibits a higher volumetric methane storage capacity of 247 cm^3 (STP) cm^{-3} and a working capacity of 186 cm^3 (STP) cm^{-3} (at 298 K and 65 bar) than 237 cm^3 (STP) cm^{-3} and 181 cm^3 (STP) cm^{-3} of NOTT-101a, attributed to the higher polarity/dipole moment of C–F bonds compared to that of C–H bonds for the enhanced electrostatic interaction with methane molecules.

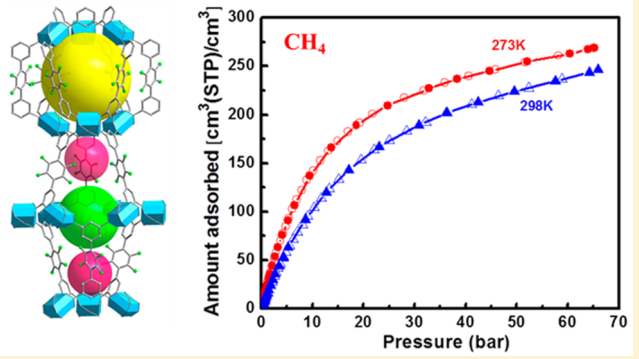

INTRODUCTION

The demand for alternative fuels over fossil fuels is now more desirable than perhaps ever before. As a more globally distributed fuel, natural gas, consisting of nearly 95% CH_4, is attracting extensive attention to serve as a bridge fuel and help us go through the transition from crude oil to future clean/renewable energy due to its economic and environmental advantages.[1,2] However, it suffers from a low volumetric energy density (only 0.11% of that of gasoline) under standard conditions, so a densification strategy that can efficiently and safely store/deliver large amounts of methane at room temperature and moderate pressures is urgently needed. Current natural gas storage technologies of liquefaction (LNG) and compression (CNG) require extreme operating conditions, presenting cost and safety issues in passenger vehicles.[3] Adsorbed natural gas (ANG), which requires much lower pressures, will be a feasible technology for passenger vehicles in terms of both cost and safety concerns in the near future.[4]

Porous metal–organic frameworks (MOFs)[5−19] have been extensively investigated for CH_4 storage due to their high porosities and tunable pore shapes/sizes combined with easily adjustable functionalities.[20−55] Recently, BASF have realized model vehicles fuelled by methane stored inside MOF materials. Since the pioneering work on porous MOFs for methane storage by Kitagawa and Yaghi,[43−45] there has been significant progress in porous MOFs for methane storage over the past decade.[46−52] A few porous MOFs have been realized to exhibit high methane storage and some even reached the DOE's target.[53−55] For example, HKUST-1 exhibits a high volumetric methane uptake of 267 cc(STP)/cc at 298 K and 65 bar,[53] while UTSA-76 with the pyrimidine groups displays the significantly high methane working capacity of about 200 cc(STP)/cc.[54] More recently, the Long group has reported a flexible MOF Co(bdp) with a usable CH_4 capacity of 197 cc(STP)/cc,[55] which might open the door to surpass the methane storage limitation within robust MOFs.[56,57]

To optimize volumetric methane storage capacities, the ideal MOFs should have balanced porosities and framework densities. In this regard, the NbO-topology MOFs assembled from tetratopic linkers and copper paddle-wheel $Cu_2(COO)_4$ clusters are of particular interest for methane storage because of their high surface areas, tunable pore sizes, and suitable open copper(II) sites.[58−60] On the basis of these fundamental framework backbones, we speculate that introduction of additional functional sites for their enhanced interactions with methane molecules may enable us to target some new MOFs with higher methane storage capacities. Indeed, we reported

Received: March 9, 2016
Revised: April 4, 2016
Published: April 14, 2016

DOI: 10.1021/acs.cgd.6b00385
Cryst. Growth Des. 2016, 16, 3395−3399

that an isoreticular NOTT-101 with -CF_3 groups shows an enhanced methane storage capacity.[61] We speculate that the introduction of the more polar C−F bonds into the isoreticular NOTT-108 will lead to higher methane storage than its original NOTT-101 with the C−H bonds. The effect of C−F bonds within MOFs for methane storage has been barely examined so far.[62−64]

The synthesis and X-ray structure of NOTT-108 have been described previously; however, no pure single-phase NOTT-108 was obtained.[64] In the current work, we optimized the reaction conditions and were able to synthesize high purity single phase NOTT-108 and thus to examine its methane storage capacity. As expected, the resulting fluorinated MOF has the same NbO topology as NOTT-101 with the slightly lower surface area and pore volume due to the bulky fluorine atoms compared with hydrogen atoms. However, the activated NOTT-108a exhibits a higher methane storage capacity of 247 cm^3 (STP) cm^{-3} (at 298 K and 65 bar) and a working capacity of 186 cm^3 (STP) cm^{-3} than 237 cm^3 (STP) cm^{-3} and 181 cm^3 (STP) cm^{-3} of NOTT-101a, attributed to the higher polarity/dipole moment of C−F bonds compared to that of C−H bonds for the enhanced electrostatic interaction with methane molecules. Accordingly, NOTT-108a is another promising MOF with high methane storage and working capacities.

Scheme 1. Schematic Structure of the Organic Ligands for the Construction of (a) NOTT-101 and (b) NOTT-108

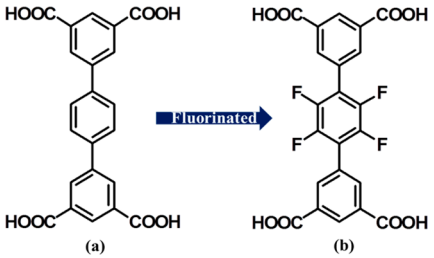

EXPERIMENTAL SECTION

Materials and Measurements. All reagents and solvents were commercially available and used without further purification. The fluorinated ligand 2′,3′,5′,6′-tetrafluoro-[1,1′:4′,1″-terphenyl]-3,3″,5,5″-tetracarboxylic acid (H_4L) was prepared according to previously published procedures.[64] Elemental analyses were performed with a PerkinElmer 240 CHN analyzer. Thermogravimetric analysis (TGA) was carried out using a Shimadzu TGA-50 analyzer under a nitrogen atmosphere, with a heating rate of 3 °C min^{-1}. Powder X-ray diffraction (PXRD) patterns were measured by a Rigaku Ultima IV diffractometer operated at 40 kV and 44 mA with a scan rate of 1.0 deg min^{-1}.

Gas Adsorption Measurements. A Micromeritics ASAP 2020 surface area analyzer was used to measure gas adsorption isotherms. To remove all the guest solvents in the framework, the fresh sample of NOTT-108 was guest-exchanged with dry acetone at least 10 times, filtered, and degassed at room temperature for 1 day and then at 373 K for another 12 h until the outgas rate was 5 mmHg min^{-1} before the measurements were made. High-pressure CH_4 and CO_2 sorption isotherms were measured using a Sieverts-type apparatus. A detailed description of the experimental setup, calibration, and isotherm has been published previously.[65]

Synthesis of NOTT-108. A mixture of the organic linker H_4L (10 mg, 0.021 mmol) and $Cu(NO_3)_2{\cdot}2.5H_2O$ (20.0 mg, 0.086 mmol) was dissolved into a mixed solvent (DMF/MeCN/H_2O, 5 mL/1 mL/1 mL) in a screw-capped vial (20 mL), to which 50 μL of 37% HCl was added. The vial was capped and heated in an oven at 85 °C for 48 h. Blue block crystals were obtained by filtration and washed with DMF several times to afford NOTT-108 in 65% yield. NOTT-108 has a best formula as $[Cu_2L(H_2O)_2]{\cdot}5DMF{\cdot}3H_2O$, which was obtained based on single-crystal X-ray structure determination, elemental analysis and TGA. Anal. Calcd for $C_{37}H_{51}N_5F_4O_{18}Cu_2$: C, 42.05; H, 4.86; N, 6.63; found: C, 43.08; H, 4.71; N, 6.72. TGA data (Figure S1) for loss of 5DMF and 5H_2O: calcd: 43.1%, found: 42.8%.

RESULTS AND DISCUSSION

A solvothermal reaction between the organic linker and $Cu(NO_3)_2{\cdot}2.5H_2O$ in a mixed solvent of DMF/CH_3CN/H_2O under acidic conditions at 85 °C for 2 days afforded single pure-phase crystals of NOTT-108. Previously, Lin et al. did not

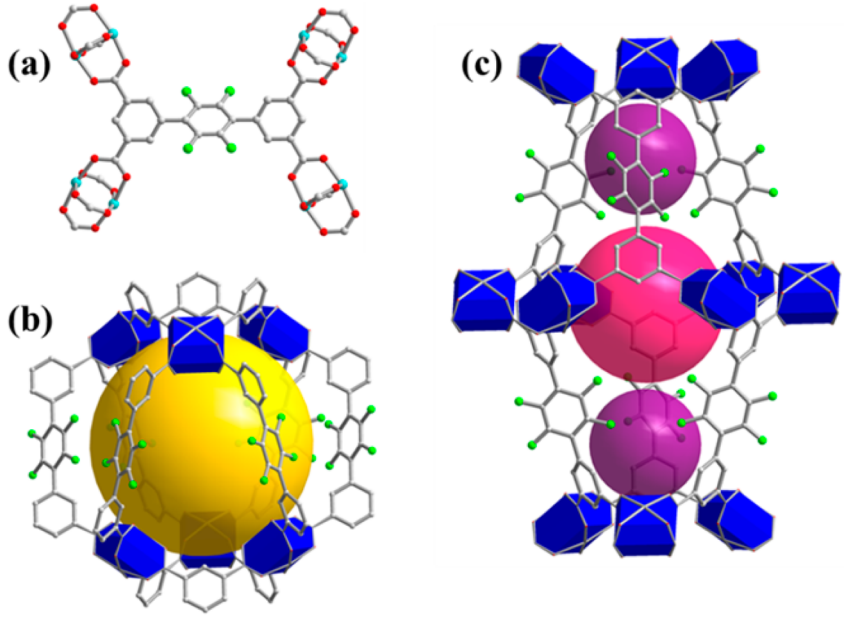

Figure 1. Crystal structure of NOTT-108: (a) each ligand coordinate four SBUs; (b) a spherical-like cage of about 9.8 Å in diameter; (c) an irregular elongated cage of about 9.4 × 22.3 Å (Cu: blue; C: gray; O: red; F: green).

DOI: 10.1021/acs.cgd.6b00385
Cryst. Growth Des. 2016, 16, 3395−3399

get the pure single-phase material, and no detailed gas sorption studies has been carried out.[64] By comparing the synthesis method with that published by Lin et al, we found that the addition of acid (HCl) was necessary for us to get single pure-phase crystals of NOTT-108, and addition of MeCN can improve the crystal quality. As shown in Figure S2, the phase purity of NOTT-108 was well confirmed by matching the experimental and simulated powder X-ray diffraction patterns, elemental analysis, and TGA studies.

As revealed, NOTT-108 crystallizes in the $R\bar{3}m$ space group and is isoreticular to NOTT-101.[64] As shown in Figure 1, the framework of NOTT-108 is built from paddlewheel dinuclear $Cu_2(COO)_4$ secondary building units (SBUs) which are connected by the carboxylates of L^{4-} to form a three-dimensional (3D) NbO-type topology. Typically, there are two types of cage in the NOTT-108 framework which are alternately stacked along the *c* axis: One cage (yellow) of about 9.8 Å in diameter and the other large irregular elongated cage of about 9.4 × 22.3 $Å^2$ which can be divided into three small cages: one squashed cuboctahedral cage at the center (pink) and two extraordinarily small cages of 3.8 Å on the top and bottom (purple).

The permanent porosity of NOTT-108 was investigated by N_2 adsorption experiments at 77 K. Before gas sorption analysis, the as-synthesized NOTT-108 was solvent-exchanged with dry acetone and evacuated at room temperature for 24 h and then heated at 373 K under a high vacuum to yield fully activated NOTT-108a. As shown in Figure 2, the N_2 sorption isotherm at 77 K indicates that NOTT-108a displays a fully reversible Type-I sorption isotherms with a saturated N_2 uptake of 620 cm^3 g^{-1}. Accordingly, NOTT-108a has a BET surface area of 2545 m^2 g^{-1} and a pore volume of 0.96 cm^3 g^{-1}. Different from the trifluoromethyl group in UTSA-88,[61] which is significantly bulky than a fluorine atom and therefore largely reduces the BET surface area and pore volume, the introduction of fluorine substituents only slightly decreases the diameter of the two types of cage, and thus porosity when compared with NOTT-101a.

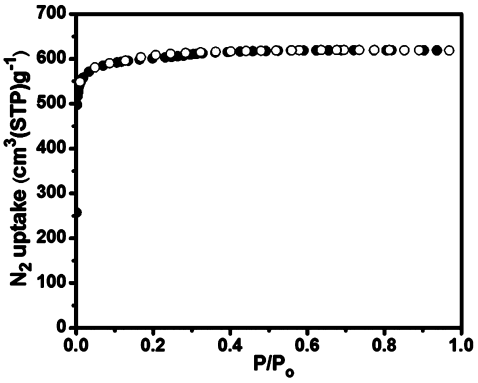

Figure 2. N_2 sorption isotherms of NOTT-108a at 77 K. Solid symbols: adsorption, open symbols: desorption.

The isoreticular pore structure and comparable porosity of NOTT-108 to that of NOTT-101 prompt us to examine its potential application in methane storage and make it possible to investigate the effect of immobilized fluorine sites on methane storage. The total volumetric methane sorption isotherms of NOTT-108a at 273 and 298 K are shown in Figure 3a. NOTT-108a has a total volumetric methane storage capacity of 201 cm^3 (STP) cm^{-3} at 298 K and 35 bar. This capacity far exceeds the DOE's previous target of 180 cm^3 (STP) cm^{-3}, while the packing density loss is ignored. When the pressure increases to 65 bar, the volumetric methane storage capacity of NOTT-108a reaches up to 247 cm^3 (STP) cm^{-3}. Comparatively, NOTT-108a shows a notably high volumetric methane storage capacity than that of NOTT-101a (237 cm^3 (STP) cm^{-3}). As shown in Table 1, NOTT-108a is also among a few MOFs exhibiting high volumetric methane storage capacities. Its gravimetric methane storage capacity of 0.226 g g^{-1} is moderately high as well.

Working capacity (also called delivery capacity), typically defined as the difference in uptake between 5 and 65 bar, is more valuable than the total storage capacity as it determines the driving range of vehicles powered by natural gas. The working capacity of NOTT-108a at 298 K is 186 cm^3 (STP) cm^{-3}, which is higher than 181 cm^3 (STP) cm^{-3} of NOTT-101a. NOTT-108a has been listed as the few MOFs with both high volumetric methane storage and working capacities, as clearly shown in Table 1.

The exceptionally high methane storage capacity and working capacity of NOTT-108a are very encouraging as it indicates that the immobilized fluorine sites might play an important role in enhancing the methane storage performance. To get better insight into the origin accounting for the resultant enhanced methane storage capacity of NOTT-108a, we first calculated the isosteric adsorption heats of methane from the temperature-dependent isotherms using the virial method. As shown in Figure S9, the initial Q_{st} of CH_4 adsorption in NOTT-

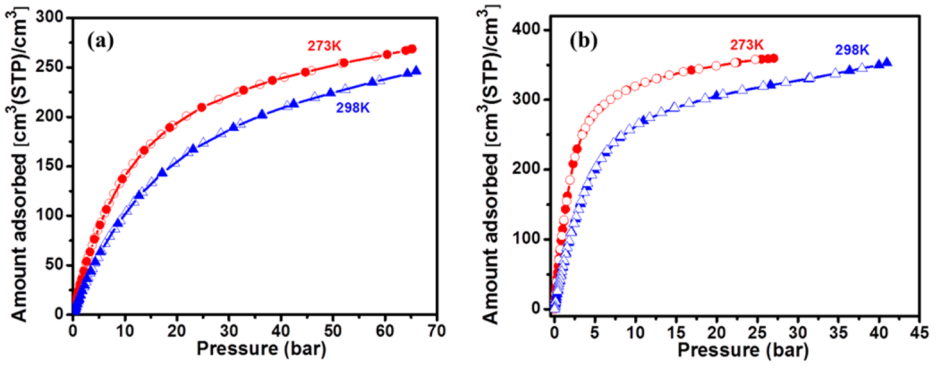

Figure 3. Total high-pressure CH_4 (a) and CO_2 (b) sorption isotherms of NOTT-108a at 273 K (red) and 298 K (blue). The filled and open symbols represent adsorption and desorption, respectively.

DOI: 10.1021/acs.cgd.6b00385
Cryst. Growth Des. 2016, 16, 3395−3399

Table 1. Comparison of Some MOFs for High-Pressure Methane Storage

MOFs	S_{BET} $m^2\ g^{-1}$	V_p $cm^3\ g^{-1}$	total uptake at 65 bar (35 bar) $g\ g^{-1}$	total uptake at 65 bar (35 bar) $cm^3\ cm^{-3}$	working capacity at 65 bar (35 bar) $cm^3\ cm^{-3}$	initial Q_{st}
NOTT-108a	2545	0.96	0.226 (0.184)	247 (201)	186 (140)	16.8
HKUST-1[53]	1850	0.78	0.216 (0.184)	267 (227)	190 (150)	17.0
UTSA-76a[54]	2820	1.09	0.263 (0.216)	257(211)	197(151)	15.4
Co(bdp)[55]	2670	0.93		203(161)	197(155)	
NOTT-101a[59]	2805	1.08	0.247 (0.202)	237 (194)	181 (138)	15.5
ZJU-5a[58]	2823	1.07	0.240 (0.200)	228 (190)	168 (130)	15.3
NU-125[53]	3120	1.29	0.287 (0.225)	232 (182)	183 (133)	15.1
UTSA-88a[61]	1771	0.68	0.206 (0.169)	248 (204)	185 (141)	15.1
PCN-14[50]	1984	0.83	0.204 (0.172)	239 (202)	160 (125)	18.7
UTSA-20a[53]	1620	0.66	0.181 (0.145)	230 (184)	170 (124)	18.2
NU-111[53]	4930	2.09	0.360 (0.241)	206 (138)	179 (111)	14.2
ZJNU-50a[60]	3308	1.18	0.274 (0.213)	229 (178)	184 (133)	15.0
UTSA-80a[51]	2280	1.03	0.240 (0.198)	233 (192)	174 (133)	15.9

108a is 16.8 kJ mol^{-1}, which is relatively higher than that of NOTT-101a (15.5 kJ mol^{-1}), and is thus responsible for the slightly increased methane uptake at low pressure. Actually, this increment in Q_{st} can be viewed as a slight enhancement over most nonfluorinated NbO-type series MOFs (Table 1), whose initial Q_{st} generally falls into the range from 15 kJ mol^{-1} to 16 kJ mol^{-1}, but significantly lower than those with strong interactions between methane and the framework, e.g., Ni-MOF-74 (~21 kJ mol^{-1}) and PCN-14 (~19 kJ mol^{-1}).[53] As previously reported,[66,67] at low pressure, the gas uptake in the MOF structure is dominated by strong adsorption on primary binding sites (e.g., the open Cu sites). At high pressure, adsorption on secondary adsorption sites (e.g., the organic linker surface) may also contribute significantly to the total gas uptake. Accordingly, we performed dispersion-corrected density-functional theory (DFT-D) calculations[68] and found that the static binding energies of CH_4 on the fluorinated center linker ring (16.4 kJ/mol) are ~10% stronger than those on the phenyl ring. The significant polarity/dipole moment of C−F bond provides enhanced electrostatic interaction with the CH_4 molecules. Such improved secondary adsorption explains well the much higher CH_4 uptakes at high pressure in NOTT-108a in comparison to NOTT-101a.

High pressure CO_2 adsorption isotherms (0−40 bar) were also performed at various temperatures. As shown in Figure 3b, NOTT-108a shows a notably high volumetric CO_2 uptake of 330 cm^3 (STP) cm^{-3} (18.9 mmol/g) at 298 K and 30 bar, which is among the few best performing MOFs with CO_2 uptake over 320 cm^3 (STP) cm^{-3}.[69] The corresponding Q_{st} at zero coverage is calculated to be 23.7 kJ mol^{-1}, slightly higher than that of NOTT-101a (23.2 kJ mol^{-1}).[70]

In summary, a fluorinated metal−organic framework NOTT-108 with single pure-phase has been synthesized for the first time. The activated NOTT-108a shows a moderate high permanent porosity, which is comparable to its isoreticular NOTT-101a. Importantly, NOTT-108a shows a much enhanced volumetric methane storage capacity of 247 cm^3 (STP) cm^{-3} (at 298 K and 65 bar) and a working capacity of 186 cm^3 (STP) cm^{-3} in comparison with the isoreticular NOTT-101a, highlighting NOTT-108a as the few MOFs with both high volumetric methane storage and working capacities. Such enhanced methane storage capacities are attributed to the higher polarity/dipole moment of C−F bonds compared to that of C−H bonds, which provides enhanced electrostatic interaction with the methane molecules. This work might motivate more extensive research to develop new MOFs with enhanced methane storage capacities through the introduction of some specific adsorption sites on the pore surfaces for their stronger interactions with methane molecules.

■ ASSOCIATED CONTENT

Supporting Information

The Supporting Information is available free of charge on the ACS Publications website at DOI: 10.1021/acs.cgd.6b00385.

TGA, PXRD, gas sorption isotherm, calculation of BET surface area of NOTT-108, the isosteric enthalpy of adsorption (PDF)

■ AUTHOR INFORMATION

Corresponding Authors

*E-mail: bin.li@utsa.edu.
*E-mail: baozb@zju.edu.cn.
*E-mail: banglin.chen@utsa.edu.

Notes

The authors declare no competing financial interest.

■ ACKNOWLEDGMENTS

This work was supported by an award AX-1730 from the Welch Foundation (B.C.), the National Natural Science Foundation of China (Nos. 21436010 and 21376205), and Lin Guangzhao & Hu Guozan Graduate Education International Exchange fund.

■ REFERENCES

(1) Service, R. F. *Science* **2014**, *346*, 538.
(2) Alvarez, R. A.; Pacala, S. W.; Winebrake, J. J.; Chameides, W. L.; Hamburg, S. P. *Proc. Natl. Acad. Sci. U. S. A.* **2012**, *109*, 6435.
(3) Yeh, S. *Energy Policy* **2007**, *35*, 5865.
(4) Wegrzyn, J.; Gurevich, M. *Appl. Energy* **1996**, *55*, 71.
(5) Furukawa, H.; Cordova, K. E.; O'Keeffe, M.; Yaghi, O. M. *Science* **2013**, *341*, 1230444.
(6) Hu, Z.; Deibert, B. J.; Li, J. *Chem. Soc. Rev.* **2014**, *43*, 5815.
(7) Zhang, J. P.; Zhang, Y. B.; Lin, J. B.; Chen, X. M. *Chem. Rev.* **2012**, *112*, 1001.
(8) He, Y.; Li, B.; O'Keeffe, M.; Chen, B. *Chem. Soc. Rev.* **2014**, *43*, 5618.
(9) Sumida, K.; Rogow, D. L.; Mason, J. A.; McDonald, T. M.; Bloch, E. D.; Herm, Z. R.; Bae, T. H.; Long, J. R. *Chem. Rev.* **2012**, *112*, 724.
(10) Eddaoudi, M.; Sava, D. F.; Eubank, J. F.; Adil, K.; Guillerm, V. *Chem. Soc. Rev.* **2015**, *44*, 228.

DOI: 10.1021/acs.cgd.6b00385
Cryst. Growth Des. 2016, 16, 3395−3399

(11) Suh, M. P.; Park, H. J.; Prasad, T. K.; Lim, D. W. *Chem. Rev.* **2012**, *112*, 782.
(12) Zhu, Q. L.; Xu, Q. *Chem. Soc. Rev.* **2014**, *43*, 5468.
(13) Nugent, P.; Belmabkhout, Y.; Burd, S. D.; Cairns, A. J.; Luebke, R.; Forrest, K.; Pham, T.; Ma, S.; Space, B.; Wojtas, L. M.; Zaworotko, M. J.; Eddaoudi, M. J. *Nature* **2013**, *495*, 80.
(14) Cui, Y. J.; Li, B.; He, H. J.; Zhou, W.; Chen, B.; Qian, G. D. *Acc. Chem. Res.* **2016**, *49*, 483.
(15) Ferey, G.; Serre, C. *Chem. Soc. Rev.* **2009**, *38*, 1380.
(16) Zheng, S. T.; Wu, T.; Chou, C.; Fuhr, A.; Feng, P.; Bu, X. *J. Am. Chem. Soc.* **2012**, *134*, 4517.
(17) Li, B.; Zhang, Y.; Ma, D.; Ma, T.; Shi, Z.; Ma, S. *J. Am. Chem. Soc.* **2014**, *136*, 1202.
(18) Dutta, A.; Koh, K.; Wong-Foy, A. G.; Matzger, A. J. *Angew. Chem., Int. Ed.* **2015**, *54*, 3983.
(19) Zheng, B.; Bai, J.; Duan, J.; Wojtas, L.; Zaworotko, M. J. *J. Am. Chem. Soc.* **2011**, *133*, 748.
(20) Makal, T. A.; Li, J. R.; Lu, W.; Zhou, H. C. *Chem. Soc. Rev.* **2012**, *41*, 7761.
(21) Li, B.; Wen, H. M.; Zhou, W.; Chen, B. *J. Phys. Chem. Lett.* **2014**, *5*, 3468.
(22) Mason, J. A.; Veenstra, M.; Long, J. R. *Chem. Sci.* **2014**, *5*, 32.
(23) He, Y.; Zhou, W.; Qian, G.; Chen, B. *Chem. Soc. Rev.* **2014**, *43*, 5657.
(24) Peng, Y.; Srinivas, G.; Wilmer, C. E.; Eryazici, I.; Snurr, R. Q.; Hupp, J. T.; Yildirim, T.; Farha, O. K. *Chem. Commun.* **2013**, *49*, 2992.
(25) Kim, H.; Samsonenko, D. G.; Das, S.; Kim, G. H.; Lee, H. S.; Dybtsev, D. N.; Berdonosova, E. A.; Kim, K. *Chem. - Asian J.* **2009**, *4*, 886.
(26) Chowdhury, P.; Mekala, S.; Dreisbach, F.; Gumma, S. *Microporous Mesoporous Mater.* **2012**, *152*, 246.
(27) Wiersum, A. D.; Chang, J. S.; Serre, C.; Llewellyn, P. L. *Langmuir* **2013**, *29*, 3301.
(28) Cavenati, S.; Grande, C. A.; Rodrigues, A. E. *Ind. Eng. Chem. Res.* **2008**, *47*, 6333.
(29) Xiang, Z.; Hu, Z.; Cao, D.; Yang, W.; Lu, J.; Han, B.; Wang, W. *Angew. Chem., Int. Ed.* **2011**, *50*, 491.
(30) Lu, Z.; Du, L.; Tang, K.; Bai, J. *Cryst. Growth Des.* **2013**, *13*, 2252.
(31) Liu, D.; Wu, H.; Wang, S.; Xie, Z.; Li, J.; Lin, W. *Chem. Sci.* **2012**, *3*, 3032.
(32) Wang, Y.; Tan, C.; Sun, Z.; Xue, Z.; Zhu, Q.; Shen, C.; Wen, Y.; Hu, S.; Wang, Y.; Sheng, T.; Wu, X. *Chem. - Eur. J.* **2014**, *20*, 1341.
(33) Zhao, X.; Sun, D.; Yuan, S.; Feng, S.; Cao, R.; Yuan, D.; Wang, S.; Dou, J.; Sun, D. *Inorg. Chem.* **2012**, *51*, 10350.
(34) Wang, Z.; Zheng, B.; Liu, H.; Lin, X.; Yu, X.; Yi, P.; Yun, R. *Cryst. Growth Des.* **2013**, *13*, 5001.
(35) Li, L.; Tang, S.; Wang, C.; Lv, X.; Jiang, M.; Wu, H.; Zhao, X. *Chem. Commun.* **2014**, *50*, 2304.
(36) Pang, J.; Jiang, F.; Wu, M.; Yuan, D.; Zhou, K.; Qian, J.; Su, K.; Hong, M. *Chem. Commun.* **2014**, *50*, 2834.
(37) Noro, S. I.; Kitagawa, S.; Kondo, M.; Seki, K. *Angew. Chem., Int. Ed.* **2000**, *39*, 2081.
(38) Feldblyum, J. I.; Dutta, D.; Wong-Foy, A. G.; Dailly, A.; Imirzian, J.; Gidley, D. W.; Matzger, A. J. *Langmuir* **2013**, *29*, 8146.
(39) Hou, C.; Liu, Q.; Fan, J.; Zhao, Y.; Wang, P.; Sun, W. Y. *Inorg. Chem.* **2012**, *51*, 8402.
(40) Klein, N.; Senkovska, I.; Gedrich, K.; Stoeck, U.; Henschel, A.; Mueller, U.; Kaskel, S. *Angew. Chem., Int. Ed.* **2009**, *48*, 9954.
(41) Loiseau, T.; Lecroq, L.; Volkringer, C.; Marrot, J.; Ferey, G.; Haouas, M.; Taulelle, F.; Bourrelly, S.; Llewellyn, P. L.; Latroche, M. *J. Am. Chem. Soc.* **2006**, *128*, 10223.
(42) Guo, Z.; Cao, R.; Wang, X.; Li, H.; Yuan, W.; Wang, G.; Wu, H.; Li, J. *J. Am. Chem. Soc.* **2009**, *131*, 6894.
(43) Kondo, M.; Yoshitomi, T.; Seki, K.; Matsuzaka, H.; Kitagawa, S. *Angew. Chem., Int. Ed. Engl.* **1997**, *36*, 1725.
(44) Noro, S. i.; Kitagawa, S.; Kondo, M.; Seki, K. *Angew. Chem., Int. Ed.* **2000**, *39*, 2081.
(45) Eddaoudi, M.; Kim, J.; Rosi, N.; Vodak, D.; Wachter, J.; O'Keeffe, M.; Yaghi, O. M. *Science* **2002**, *295*, 469.
(46) Li, B.; Wen, H.; Wang, H.; Wu, H.; Yildirim, T.; Zhou, W.; Chen, B. *Energy Environ. Sci.* **2015**, *8*, 2504.
(47) Wilmer, C. E.; Farha, O. K.; Yildirim, T.; Eryazici, I.; Krungleviciute, V.; Sarjeant, A. A.; Snurr, R. Q.; Hupp, J. T. *Energy Environ. Sci.* **2013**, *6*, 1158.
(48) Guo, Z.; Wu, H.; Srinivas, G.; Zhou, Y.; Xiang, S.; Chen, Z.; Yang, Y.; Zhou, W.; O'Keeffe, M.; Chen, B. *Angew. Chem., Int. Ed.* **2011**, *50*, 3178.
(49) Gándara, F.; Furukawa, H.; Lee, S.; Yaghi, O. M. *J. Am. Chem. Soc.* **2014**, *136*, 5271.
(50) Ma, S.; Sun, D.; Simmons, J. M.; Collier, C. D.; Yuan, D.; Zhou, H. C. *J. Am. Chem. Soc.* **2008**, *130*, 1012.
(51) Wen, H.; Li, B.; Yuan, D.; Wang, H.; Yildirim, T.; Zhou, W.; Chen, B. *J. Mater. Chem. A* **2014**, *2*, 11516.
(52) Spanopoulos, I.; Tsangarakis, C.; Klontzas, E.; Tylianakis, E.; Froudakis, G.; Adil, K.; Belmabkhout, Y.; Eddaoudi, M.; Trikalitis, P. *J. Am. Chem. Soc.* **2016**, *138*, 1568.
(53) Peng, Y.; Krungleviciute, V.; Eryazici, I.; Hupp, J. T.; Farha, O. K.; Yildirim, T. *J. Am. Chem. Soc.* **2013**, *135*, 11887.
(54) Li, B.; Wen, H.; Wang, H.; Wu, H.; Tyagi, M.; Yildirim, T.; Zhou, W.; Chen, B. *J. Am. Chem. Soc.* **2014**, *136*, 6207.
(55) Mason, J. A.; Oktawiec, J.; Taylor, M. K.; Hudson, M. R.; Rodriguez, J.; Bachman, J. E.; Gonzalez, M. I.; Cervellino, A.; Guagliardi, A.; Brown, C. M.; Llewellyn, P. L.; Masciocchi, N.; Long, J. R. *Nature* **2015**, *527*, 357.
(56) Simon, C. M.; Kim, J.; Gomez-Gualdron, D. A.; Camp, J. S.; Chung, Y. G.; Martin, R. L.; Mercado, R.; Deem, M. W.; Gunter, D.; Haranczyk, M.; Sholl, D. S.; Snurr, R. Q.; Smit, B. *Energy Environ. Sci.* **2015**, *8*, 1190.
(57) Gómez-Gualdrón, D. A.; Wilmer, C. E.; Farha, O. K.; Hupp, J. T.; Snurr, R. Q. *J. Phys. Chem. C* **2014**, *118*, 6941.
(58) Rao, X.; Cai, J.; Yu, J.; He, Y.; Wu, C.; Zhou, W.; Yildirim, T.; Chen, B.; Qian, G. *Chem. Commun.* **2013**, *49*, 6719.
(59) He, Y.; Zhou, W.; Yildirim, T.; Chen, B. *Energy Environ. Sci.* **2013**, *6*, 2735.
(60) Song, C.; Ling, Y.; Feng, Y.; Zhou, W.; Yildirim, T.; He, Y. *Chem. Commun.* **2015**, *51*, 8508.
(61) Chang, G.; Li, B.; Wang, H.; Bao, Z.; Yildirim, T.; Yao, Z.; Xiang, S.; Zhou, W.; Chen, B. *Chem. Commun.* **2015**, *51*, 14789.
(62) Yang, C.; Wang, X.; Omary, M. A. *J. Am. Chem. Soc.* **2007**, *129*, 15454.
(63) Pachfule, P.; Chen, Y.; Jiang, J.; Banerjee, R. *Chem. - Eur. J.* **2012**, *18*, 688.
(64) Lin, X.; Telepeni, I.; Blake, A. J.; Dailly, A.; Brown, C. M.; Simmons, J. M.; Zoppi, M.; Walker, G. S.; Thomas, K. M.; Mays, T. J.; Hubberstey, P.; Champness, N. R.; Schröder, M. *J. Am. Chem. Soc.* **2009**, *131*, 2159.
(65) Zhou, W.; Wu, H.; Hartman, M. R.; Yildirim, T. *J. Phys. Chem. C* **2007**, *111*, 16131.
(66) Wu, H.; Zhou, W.; Yildirim, T. *J. Am. Chem. Soc.* **2009**, *131*, 4995.
(67) Wu, H.; Simmons, J. M.; Liu, Y.; Brown, C. M.; Wang, X. S.; Ma, S.; Peterson, V. K.; Southon, P. D.; Kepert, C. J.; Zhou, H. C.; Yildirim, T.; Zhou, W. *Chem. - Eur. J.* **2010**, *16*, 5205.
(68) Giannozzi, P.; Baroni, S.; Bonini, N.; Calandra, M.; Car, R.; Cavazzoni, C.; Ceresoli, D.; Chiarotti, G. L.; Cococcioni, M.; Dabo, I.; Dal Corso, A.; Fabris, S.; Fratesi, G.; de Gironcoli, S.; Gebauer, R.; Gerstmann, U.; Gougoussis, C.; Kokalj, A.; Lazzeri, M.; Martin-Samos, L.; Marzari, N.; Mauri, F.; Mazzarello, R.; Paolini, S.; Pasquarello, A.; Paulatto, L.; Sbraccia, C.; Scandolo, S.; Sclauzero, G.; Seitsonen, A. P.; Smogunov, A.; Umari, P.; Wentzcovitch, R. M. *J. Phys.: Condens. Matter* **2009**, *21*, 395502.
(69) Zhang, Z.; Yao, Z.; Xiang, S.; Chen, B. *Energy Environ. Sci.* **2014**, *7*, 2868.
(70) Song, C.; He, Y.; Li, B.; Ling, Y.; Wang, H.; Feng, Y.; Krishna, R.; Chen, B. *Chem. Commun.* **2014**, *50*, 12105.

DOI: 10.1021/acs.cgd.6b00385
Cryst. Growth Des. 2016, 16, 3395−3399